

Article

# Milliwatt-Level Spontaneous Emission Across the 3.5–8 $\mu\text{m}$ Spectral Region from $\text{Pr}^{3+}$ Doped Selenide Chalcogenide Fiber Pumped with a Laser Diode

Lukasz Sojka <sup>1</sup>, Zhuoqi Tang <sup>2</sup>, Dinuka Jayasuriya <sup>2,†</sup>, Meili Shen <sup>2</sup>, Joel Nunes <sup>2</sup>, David Furniss <sup>2</sup>, Mark Farries <sup>2</sup> , Trevor M. Benson <sup>2</sup>, Angela B. Seddon <sup>2</sup> and Slawomir Sujecki <sup>1,2,\*</sup> 

<sup>1</sup> Department of Telecommunications and Teleinformatics, Faculty of Electronics, Wrocław University of Science and Technology, Wybrzeże Wyspińskiego 27, 50-370 Wrocław, Poland; lukasz.sojka@pwr.edu.pl

<sup>2</sup> Mid-Infrared Photonics Group, George Green Institute for Electromagnetics Research, Faculty of Engineering, University of Nottingham, University Park, Nottingham NG7 2RD, UK; Zhuoqi.Tang@nottingham.ac.uk (Z.T.); Dinuka.Jayasuriya@nottingham.ac.uk (D.J.); Meili.Shen@nottingham.ac.uk (M.S.); eexjn6@exmail.nottingham.ac.uk (J.N.); emzdf@exmail.nottingham.ac.uk (D.F.); ezamf3@exmail.nottingham.ac.uk (M.F.); trevor.benson@nottingham.ac.uk (T.M.B.); emzabs@exmail.nottingham.ac.uk (A.B.S.)

\* Correspondence: slawomir.sujecki@pwr.edu.pl or slawomir.sujecki@nottingham.ac.uk

† Now at ThorLabs, 1 St. Thomas Place, Ely CB7 4EX, UK.

Received: 15 December 2019; Accepted: 7 January 2020; Published: 11 January 2020



**Featured Application:** A candidate for the realization of a broadband mid-infrared spontaneous emission fiber source for biological and medical applications is demonstrated.

**Abstract:** A spontaneous emission fiber source operating in the mid-infrared (MIR) wavelength range from 3.5 to 8  $\mu\text{m}$  is demonstrated for the first time at output power levels of at least 1 mW. The source is a  $\text{Pr}^{3+}$ -doped selenide chalcogenide, multimode, glass fiber pumped with commercially available laser diodes operating at 1.470  $\mu\text{m}$ , 1.511  $\mu\text{m}$  and 1.690  $\mu\text{m}$ . This MIR spontaneous emission fiber source offers a viable alternative to broadband mid-infrared supercontinuum fiber sources, which are comparatively complex and costly. The MIR emission wavelength range is significant for molecular sensing applications across biology and chemistry, and in medicine, agriculture, defense, and environmental monitoring.

**Keywords:** mid-infrared light sources; chalcogenide glass fibers; mid-infrared; fiber lasers

## 1. Introduction

Mid-infrared (MIR) fiber sources have been the subject of extensive research in recent years. The main reason is the broad range of potential applications for such sources in fields of biomedical sensing, environmental monitoring, free space communication and so on [1–5]. When compared to other types of MIR light sources, fiber sources have advantages of good beam quality, compactness, reliability, and a simple construction [1–5]. Recently, continuous wave (CW) 3.92  $\mu\text{m}$  laser action at room temperature has been observed in  $\text{Ho}^{3+}$ -doped fluoroindate glass fibers [6] and photoluminescence beyond 4  $\mu\text{m}$  in  $\text{Dy}^{3+}$ -doped fluoroindate glass fibers [7]. Bearing in mind that it has taken 23 years to push the fiber lasing wavelength from 3.90  $\mu\text{m}$  [8] only to 3.92  $\mu\text{m}$  i.e., [6], to access longer wavelengths, beyond 4  $\mu\text{m}$ , host glass materials with lower phonon energy are needed [5]. Potentially excellent candidate host glasses are chalcogenide-selenide glasses. Chalcogenide-selenide glass fibers have already proven their usefulness in the development of ultra-broadband MIR supercontinuum sources to 15  $\mu\text{m}$  [9,10]. In addition, Raman lasers operating beyond 3.5  $\mu\text{m}$  have been successfully realized in chalcogenide

glass fibers [11]. However, the making of lanthanide ion-doped MIR fiber lasers beyond, 4  $\mu\text{m}$  has so far proved elusive, despite large efforts. To date, spontaneous emission in the range 3–6  $\mu\text{m}$  has been observed in chalcogenide glasses doped with  $\text{Pr}^{3+}$ ,  $\text{Tb}^{3+}$ ,  $\text{Dy}^{3+}$  or  $\text{Nd}^{3+}$  [12–17]. Also, PL (photoluminescence) in bulk chalcogenide glasses has been observed in the 7–8  $\mu\text{m}$  region in  $\text{Tb}^{3+}$  and  $\text{Pr}^{3+}$ , respectively, [18,19]. Recently, spontaneous emission between 7–9  $\mu\text{m}$  has been reported in chalcogenide glass fibers doped with  $\text{Tb}^{3+}$  or  $\text{Sm}^{3+}$ , respectively [20,21]. Nonetheless, the failure to achieve MIR laser action in chalcogenide glass fibers doped with lanthanides is in part, at least, due to residual loss around 4.6  $\mu\text{m}$  wavelength because of Se-H extrinsic impurity in the glass host [22]. Still, rare earth ion-doped chalcogenide glass multimode fibers show great promise to act instead as MIR spontaneous emission fiber light sources. A MIR spontaneous emission fiber source comprises a rare earth ion-doped chalcogenide fiber, a pump laser and focusing optics. Importantly, in the case of spontaneous emission sources, a population inversion is not required. This is because the MIR light is produced via the spontaneous emission phenomenon. Work to date has shown their suitability in gas sensing [14,23–26]. Moreover, absorption bands arising from vibrational excitations relevant to biological and medical applications cover the wavelength range from 2.8 to 3.7  $\mu\text{m}$  and from 5.7 to 7.3  $\mu\text{m}$  [4] and both are covered by a MIR spontaneous emission fiber source. Further, most FTIR (Fourier transform infrared) spectrometers use as a MIR light source, a Globar. A Globar is silicon carbide rod of 5 to 10 mm width and 20 to 50 mm length that is electrically heated up to 1000 to 1650  $^{\circ}\text{C}$ . A Globar requires water-cooling and also special safety precautions. The MIR rare earth-doped spontaneous emission source developed in this contribution operates, on the other hand, at room temperature and is easy to handle.

Praseodymium ion-doped, selenide host glasses exhibit strong absorption bands at 1.55  $\mu\text{m}$  and 1.94  $\mu\text{m}$ , which are suitable for pumping with readily commercially available, high power, and cost-effective laser diodes. A simplified, energy-level diagram of  $\text{Pr}^{3+}$  in chalcogenide glass with indicated possible emission paths for wavelengths above 3  $\mu\text{m}$  is presented in Figure 1. Broadband MIR emission across the 3.5–6  $\mu\text{m}$  wavelength range from  $\text{Pr}^{3+}$ -doped chalcogenide glasses has already been reported by several research groups [12,13,27–35]. This MIR emission from  $\text{Pr}^{3+}$  ions can be attributed to emissions from several transitions that overlapped, including: ( ${}^3\text{F}_4, {}^3\text{F}_3$ ) $\rightarrow$ ( ${}^3\text{F}_2, {}^3\text{H}_6$ ), ( ${}^3\text{F}_2, {}^3\text{H}_6$ ) $\rightarrow$  ${}^3\text{H}_5$  and  ${}^3\text{H}_5$  $\rightarrow$  ${}^3\text{H}_4$ ). Results to date demonstrate the potential of  $\text{Pr}^{3+}$ -doped chalcogenide fiber to be developed into MIR spontaneous emission sources. This is the subject of this paper.

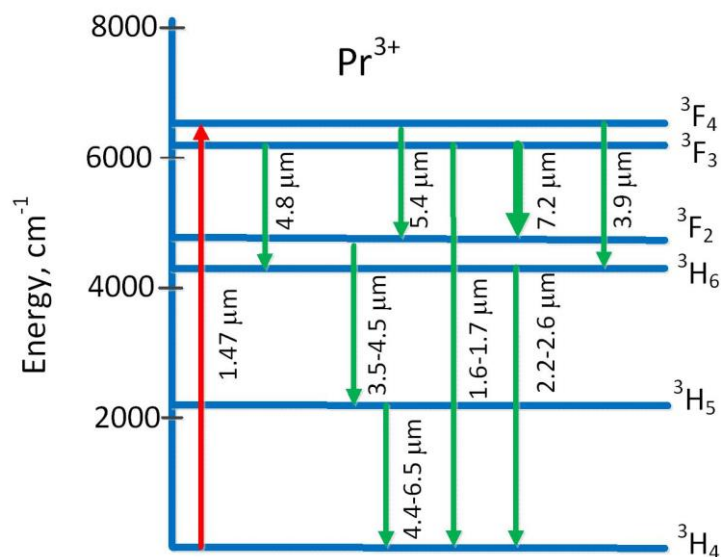


**Figure 1.** Schematic energy level diagram for  $\text{Pr}^{3+}$ -doped selenide chalcogenide with indicated possible emission paths for wavelengths above 3  $\mu\text{m}$  under 1.47  $\mu\text{m}$  pumping (adapted from [19]).

Of relevance is the recent report on MIR emission from 6.5 to 8.5  $\mu\text{m}$  in a  $\text{Pr}^{3+}$ -doped bromide crystal [36], which is attributed to the  ${}^3\text{F}_3 \rightarrow {}^3\text{F}_2$  transition. Furthermore, this emission was exploited in realizing MIR lasing in  $\text{Pr}^{3+}$ -doped crystalline materials, lasing at wavelengths: 7.2  $\mu\text{m}$  ( ${}^3\text{F}_3 \rightarrow {}^3\text{F}_2$ ), and 5.2  $\mu\text{m}$  ( ${}^3\text{F}_3 \rightarrow {}^3\text{H}_6$ ), respectively, in a  $\text{Pr}^{3+}:\text{LaCl}_3$  crystal. Such laser action utilizing the  ${}^3\text{F}_3 \rightarrow {}^3\text{F}_2$  transition exemplifies a true four-level laser system [37,38]. The maximum phonon energy of  $\text{LaCl}_3$  is around  $260\text{ cm}^{-1}$ , which is comparable to that of a chalcogenide selenide glass at  $250\text{--}300\text{ cm}^{-1}$  [39]. Despite the observation of spontaneous emission from the ( ${}^3\text{F}_4, {}^3\text{F}_3$ ) degenerate levels to the  ${}^3\text{H}_4$  ground state at ca. 1.6  $\mu\text{m}$  wavelength, which have already been reported in a  $\text{Pr}^{3+}$ -doped selenide chalcogenide glass [40–44], there is only very recent evidence for emission from this transition in the MIR region beyond 6.5  $\mu\text{m}$  in the literature to date [19]; hence, this a focus of this contribution.

The motivation of this paper is the application of praseodymium ion-doped chalcogenide selenide glass fibers, pumped using near-infrared (NIR) laser diodes, as MIR light sources. The key factors considered here are power-scaling and a large emission spectral-bandwidth. Thus, in this contribution, it is demonstrated that an output power  $> 1\text{ mW}$  in the MIR wavelength region is achievable from multimode  $\text{Pr}^{3+}$ -doped selenide chalcogenide fiber, under pumping using either 1.47  $\mu\text{m}$ , 1.51  $\mu\text{m}$  or 1.69  $\mu\text{m}$  laser diodes. To the best of our knowledge, this is the largest output power achieved to date in a rare earth ion-doped chalcogenide fiber spontaneous emission source in the spectral region beyond 3  $\mu\text{m}$ . These results clearly show the power scaling potential of the MIR spontaneous emission fiber source studied. Moreover, emission at  $\sim 7.2\text{ }\mu\text{m}$ , attributed to the  ${}^3\text{F}_3 \rightarrow {}^3\text{F}_2$  transition in the  $\text{Pr}^{3+}$  selenide chalcogenide fiber, is reported. To the best of the Authors' knowledge, this is the first experimental demonstration of 7.2  $\mu\text{m}$  emission in a  $\text{Pr}^{3+}$ -doped chalcogenide fiber, demonstrating also that the spontaneous emission from a  $\text{Pr}^{3+}$  selenide chalcogenide fiber can stretch up to 8  $\mu\text{m}$ . This is an important result from the point of view of realization of the first fiber laser beyond 4  $\mu\text{m}$ , due to the fact that the transition centered at around 7.2  $\mu\text{m}$  has the potential to operate as a four-level laser system [37].

## 2. Materials and Experimental Methods

1000 ppmw (parts per million by weight)  $\text{Pr}^{3+}$ -doped Ge-As-Ga-Se glass rods were prepared using the melt-quenching method; more details can be found in [12,29]. In the experiment, an unstructured fiber approximately 450  $\mu\text{m}$  in diameter and 70 mm long was used. The rare earth ion-doped chalcogenide glass multimode fiber fabrication is described in more detail in [12]. The experimental set-up for measuring the output power, photoluminescence (PL) spectrum and PL decay was similar to that described in [45]. The  $\text{Pr}^{3+}$ -doped selenide-chalcogenide glass fiber was placed in an aluminum V-groove on a XYZ translation stage. The output PL power was measured in the spectral region above 3  $\mu\text{m}$  by excitation of the  $\text{Pr}^{3+}$  fiber, using each of the three different laser diode pumping sources at NIR wavelengths of: 1.47  $\mu\text{m}$  (SemiNex 4PN-127), 1.511  $\mu\text{m}$  (SemiNex 4-PN-109) and 1.69  $\mu\text{m}$  (QPC Laser PR-6017-0000). For achieving efficient collection of the PL signal from the fiber end, a lens with a short focal length and high numerical aperture (NA) is preferred. This is because, due to the high refractive index of the unstructured chalcogenide glass fiber, the emitted beam divergence is large [26]. Here, three different ways of collecting PL from the fiber end were tested. In the first case: (i) the output from the fiber end was collimated using a 1.87 mm focal length (NA = 0.86) black diamond lens (Thorlabs), which was AR-(anti-reflection)-coated for the 3–5  $\mu\text{m}$  range. In case (ii), a black diamond lens was again used but the beam was subsequently focused using a germanium aspheric lens, AR-coated for 3–12  $\mu\text{m}$ , of focal length: 12.7 mm and NA = 1 (Edmund Optics Stock #89-607). In the case of (iii), a pair of germanium aspheric lenses, each of focal length: 12.7 mm, were used to collimate and then focus the light on the optical power meter detector. Germanium lenses also provided some optical filtering, with a cut-on around 2  $\mu\text{m}$ , thus the pump signal was fully attenuated before reaching the power meter. The output power was measured using a sensitive thermal power meter (Thorlabs S401C) combined with a 3  $\mu\text{m}$  cut-on long-pass filter. For measuring the PL spectra, a monochromator (MSH-150 Quantum Lot; focal length: 150 mm) operating with either a 4000-nm

blazed: 150 line/mm, or a 9000-nm blazed: 100 line/mm, grating was used. The PL was collected from the fiber end using a pair of germanium aspheric lenses, AR-coated for 3–12  $\mu\text{m}$ , of focal length = 12.7 mm and NA = 1. In this case, the pump beam was electronically chopped with a low frequency as the reference signal for a lock-in amplifier, in order to reduce any thermal background noise. The PL signal was detected in the spectral region spanning 3.0 to 9  $\mu\text{m}$ , using a thermoelectrically cooled (to 200 K) MCT (mercury cadmium telluride) detector (Vigo System PVI-4TE-8), which was connected to a lock-in amplifier (Scitec Instruments Inc., Trowbridge, UK). In the measurements, one of three long pass filters was used: a long-pass filter with cut-on wavelength around 3  $\mu\text{m}$  (Spectrogon 71M09339, Täby, Sweden), a long-pass filter with a cut-on wavelength around 3.6  $\mu\text{m}$  (Edmund Optics, Barrington, USA) or a long-pass filter with a cut-on wavelength of 6.15  $\mu\text{m}$  (Spectrogon 71M09001). The PL decay rates were measured at the fiber end using the MCT detector and directly modulating the pump lasers. The decay rates were measured at the wavelengths: 6.5  $\mu\text{m}$ , 7  $\mu\text{m}$ , and 7.4  $\mu\text{m}$ . The time response of the detector and the preamplifier used in the PL decay measurements was < 3  $\mu\text{s}$ . In order to select the measured wavelengths, a monochromator was used to act as a tunable bandpass filter. In all of the considered cases, the 6.15  $\mu\text{m}$  filter was placed in front of the monochromator to remove the pump signal and any unwanted second order diffraction. The decay at around 1.6  $\mu\text{m}$  wavelength was measured using an InGaAs photodiode, operating in the spectral range: 800–1700 nm (Thorlabs SM05PD5A, Newton, USA) coupled with a PDA200C photodiode amplifier. Note that the time response for the whole set-up was better than 5  $\mu\text{s}$ . The time evolution of the fluorescence was recorded using a digital oscilloscope (PicoScope 5442A, Cambridgeshire, UK) coupled with a PC (personal computer). Averaging was applied to reduce the noise.

### 3. Experimental Results and Discussion

In this Section, the experimental results are discussed. First the results of the power measurements are presented, followed by a discussion concerning the recorded photoluminescence spectra and luminescence lifetimes.

#### 3.1. Output Power Measurements from the $\text{Pr}^{3+}$ Doped Spontaneous Emission Fiber Source

In this subsection, the results of the output power measurements from the  $\text{Pr}^{3+}$ -doped selenide-chalcogenide glass fiber, under different pumping conditions, are presented. Figure 2 shows the measured dependence of MIR output power on the 1.47  $\mu\text{m}$  pump power. In this case, the maximum measured output power in the spectral range 3–8  $\mu\text{m}$  was around 1 mW. Measured results are very similar for all of the three different collection approaches described in Section 2, which suggests that the achieved results are repeatable and reliable. In this experiment, a 70-mm-long fiber was used. The pump absorption cross-section was around  $1.7 \times 10^{-20} \text{ cm}^2$  at 1.47  $\mu\text{m}$  and the  $\text{Pr}^{3+}$  concentration was 1000 ppmw ( $1.9 \times 10^{19} \text{ cm}^{-3}$ ) [29]; thus, 70 mm of fiber would have provided around 10 dB absorption of the 1.47  $\mu\text{m}$  pump. A longer fiber length of ~150 mm was also tested but the measured MIR output power was lower than in the case of the 70-mm-long fiber sample, which most likely can be attributed to reabsorption of the MIR output signal, plus attenuation of the output signal due to intrinsic fiber loss. Figure 3 shows the measured dependence of the MIR output power on the 1.511  $\mu\text{m}$  pump power. The results obtained for this second case were very similar to the first case when 1.47  $\mu\text{m}$  pumping was used. This can be explained by the fact that the absorption cross-section of the  $\text{Pr}^{3+}$  ions at 1.511  $\mu\text{m}$  is  $\sim 1.9 \times 10^{-20} \text{ cm}^2$ , which is very similar to their absorption cross-section at 1.47  $\mu\text{m}$ . Figure 4 presents the dependence of the output MIR power on the 1.69  $\mu\text{m}$  pump power. In this case, more pump power was needed to achieve 1 mW output power, due to the lower value of the cross-section at this wavelength, i.e.,  $0.9 \times 10^{-20} \text{ cm}^2$  at 1.69  $\mu\text{m}$ . Efficiency of approximately 0.1% implies that only a small fraction of the pump power feeds into the MIR beam collected at the end of the fiber. The remaining pump power either feeds into the generation of light at shorter wavelengths, dissipated via fiber loss, passed unabsorbed through the fiber and filtered out, or feeds into MIR emission radiated outside of the output lens aperture. To summarize these experiments,

for all considered cases, a MIR output power of, at or above 1 mW was obtained. To the Authors' best knowledge, this is the highest output power achieved from rare earth ion-doped chalcogenide fiber spontaneous emission sources in the spectral region above 3  $\mu\text{m}$ . Such broadband sources can be widely applied, for example for gas spectroscopic detection [24–26]. Further, commercially available multimode laser diodes operating at wavelengths of 1.47  $\mu\text{m}$ , 1.511  $\mu\text{m}$  and 1.69  $\mu\text{m}$  can generate output powers in the range of tens of Watts, so further power scaling of this MIR fiber spontaneous emission source is possible, considering that the pump powers used to obtain the results shown in Figures 1–3 did not exceed 2 W. In this experiment, the pump power was limited below 2 W in order to avoid possible damage of the fiber sample [46].

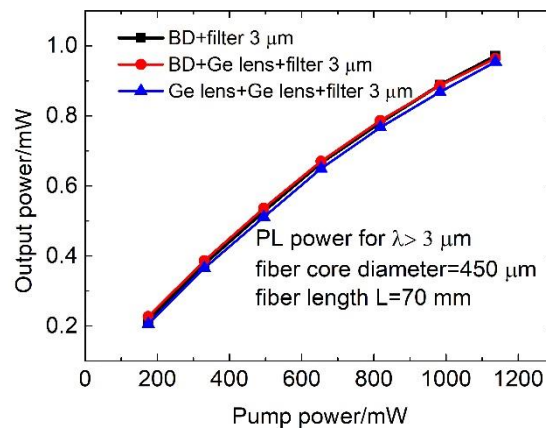


**Figure 2.** Measured dependence of MIR output power on pump power for a  $\text{Pr}^{3+}$ -doped Ge-As-Ga-Se spontaneous emission fiber source of length 70 mm. The pump wavelength was 1.47  $\mu\text{m}$ . Output power was measured after passage through a long-pass filter with cut-on at 3  $\mu\text{m}$ . BD is black diamond lens.

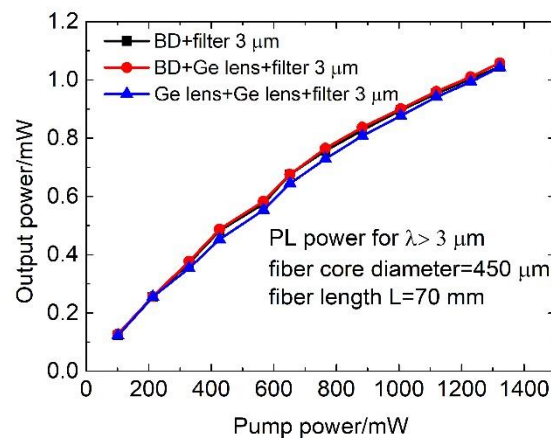


**Figure 3.** Measured dependence of MIR output power on pump power for a  $\text{Pr}^{3+}$ -doped Ge-As-Ga-Se spontaneous emission fiber source of length 70 mm. The pump wavelength was 1.511  $\mu\text{m}$ . Output power was measured after passage through a long-pass filter with cut-on at 3  $\mu\text{m}$ . BD is black diamond lens.

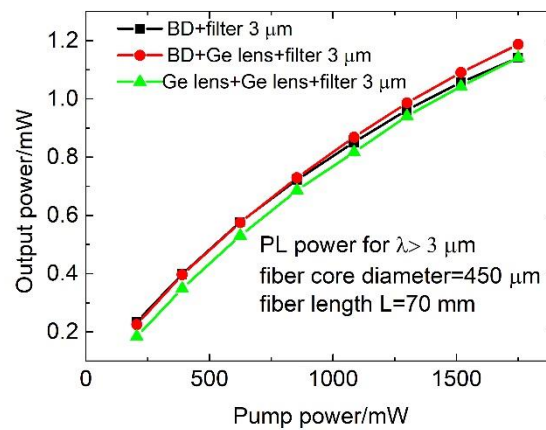


**Figure 4.** Measured dependence of MIR output power on pump power for a  $\text{Pr}^{3+}$ -doped Ge-As-Ga-Se spontaneous emission fiber source of length 70 mm. The pump wavelength was 1.69  $\mu\text{m}$ . Output power was measured after passage through a long-pass filter with cut-on at 3  $\mu\text{m}$ . BD is black diamond lens.

### 3.2. Mid-Infrared Emission from the $\text{Pr}^{3+}$ Doped Selenide-Chalcogenide Glass Fiber in the Spectral Region: 3.5–8 $\mu\text{m}$

In this subsection, the experimental investigation of the PL properties of 1000 ppmw  $\text{Pr}^{3+}$ -doped selenide-chalcogenide glass fiber is discussed. Figure 5 shows the room temperature mid-infrared emission bands of  $\text{Pr}^{3+}$ -doped GeAsGaSe glass fiber recorded in the wavelength range 3–6.5  $\mu\text{m}$  under excitation at 1.47  $\mu\text{m}$ . The PL emission was collected from the fiber end using the MCT detector operating in the spectral region 3–9  $\mu\text{m}$ , long pass filters with cut-on wavelengths of 3  $\mu\text{m}$  and 3.5  $\mu\text{m}$ , and a diffraction grating blazed at 4  $\mu\text{m}$ . The recorded emission band is mainly associated with the  $(^3\text{F}_2, ^3\text{H}_6) \rightarrow ^3\text{H}_5$  and  $^3\text{H}_5 \rightarrow ^3\text{H}_4$  transitions (see Figure 1), however, emission from  $(^3\text{F}_4, ^3\text{F}_3) \rightarrow (^3\text{F}_2, ^3\text{H}_6)$  can also contribute to the mid-infrared emission [12,19]. It can be clearly seen from Figure 5 that the emission at wavelengths longer than 6  $\mu\text{m}$  is non-negligible. Therefore, in order to investigate emissions above 6  $\mu\text{m}$ , a diffraction grating blazed at 9  $\mu\text{m}$  and a long pass filter with cut-on wavelength of 6.15  $\mu\text{m}$  were introduced into the set-up.

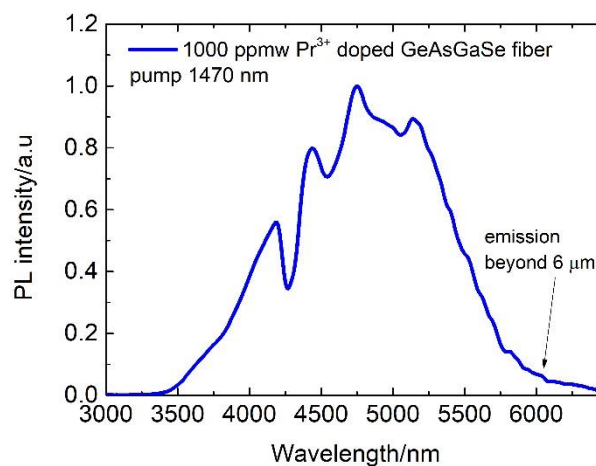


**Figure 5.** Normalized MIR PL spectrum from the 70-mm-long  $\text{Pr}^{3+}$ -doped Ge-As-Se-Ga glass fiber across the spectral region 3–6.5  $\mu\text{m}$ , pumped with a 300 mW diode laser operating at 1.47  $\mu\text{m}$ . The dip observed in the fluorescence spectra at 4.26  $\mu\text{m}$  can be attributed to ambient  $\text{CO}_2$  absorption in the optical path.

Figure 6 displays the room temperature mid-infrared emission of the 70-mm-long  $\text{Pr}^{3+}$ -doped GeAsGaSe fiber in the wavelength range: 6.15–8  $\mu\text{m}$ , under pumping at 1.47  $\mu\text{m}$ . This emission band most likely can be attributed to the long tail of the  $^3\text{H}_5 \rightarrow ^3\text{H}_4$  transition and to the emission from the

$^3F_3 \rightarrow ^3F_2$  transition (see Figure 1). Recently, a similar emission in the spectral region 6–8.5  $\mu\text{m}$  was measured in  $\text{Pr}^{3+}$ -doped bromide crystals [36] and in the bulk glass:  $\text{Pr}^{3+}$ -doped Ge-Ga-Se [19]. This emission was attributed to the  $^3F_3 \rightarrow ^3F_2$  transition [19,36]. In order to investigate further the emission across the 6.1–8  $\mu\text{m}$  spectral region in the  $\text{Pr}^{3+}$  selenide-chalcogenide glass fiber here, the PL decays at selected wavelengths were measured (see Figure 7).

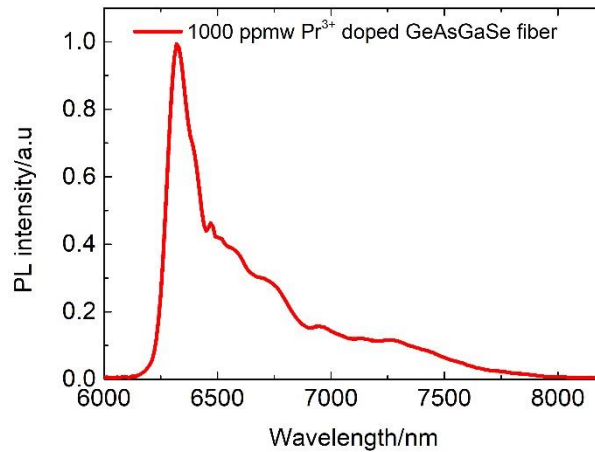


**Figure 6.** Normalized MIR PL spectrum from the 70-mm-long  $\text{Pr}^{3+}$ -doped Ge-As-Ga-Se fiber across the spectral region: 6–8  $\mu\text{m}$ , pumped with a 300 mW diode laser operating at 1.47  $\mu\text{m}$ , and the PL was measured after passage through a long-pass filter with cut-on at 6.15  $\mu\text{m}$ .

Figure 7 presents the PL decay characteristics at the output of a 70-mm-long  $\text{Pr}^{3+}$ -doped Ge-As-Ga-Se glass fiber measured at: 6.5  $\mu\text{m}$  (Figure 7a), 7  $\mu\text{m}$  (Figure 7b), 7.4  $\mu\text{m}$  (Figure 7c) and 1.6  $\mu\text{m}$  (Figure 7d), under 1.47  $\mu\text{m}$  excitation. In the measurement of PL lifetime, each presented decay plot was collected from a fiber sample and averaged over several hundred measurements to improve the signal-to-noise ratio. The measured PL decay at 6.5  $\mu\text{m}$  was best fit by using a two-exponential function. The fast decay ( $\tau_1 = 0.3$  ms) can be attributed to the  $^3F_3 \rightarrow ^3F_2$  transition whilst the slow decay  $\tau_2 = 6.8$  ms is most likely a contribution from the  $^3H_5 \rightarrow ^3H_4$  transition. From the coefficients of the calculated fitting function, one can extract that the contributed intensities at 6.5  $\mu\text{m}$  of the  $^3H_5 \rightarrow ^3H_4$  and  $^3F_3 \rightarrow ^3F_2$  transitions are in the ratio of approximately 1.3:1. In the case of the PL decay measured at 7  $\mu\text{m}$ , a similar two-exponential behavior can be observed, but in this case the  $^3H_5 \rightarrow ^3H_4$  and  $^3F_3 \rightarrow ^3F_2$  transitions 'contributed intensities' ratio was 1:1.7, while for the PL decay recorded at 7.4  $\mu\text{m}$ , the ratio of contributed intensities between the  $^3H_5 \rightarrow ^3H_4$  and  $^3F_3 \rightarrow ^3F_2$  transitions was 1:5.3. Thus, these results show that, at longer wavelengths, the contribution from the  $^3F_3 \rightarrow ^3F_2$  transition starts to dominate. In order to provide further evidence showing that the observed emission comes from the  $^3F_3$  level, the emission at 1.6  $\mu\text{m}$  wavelength was measured. The emission at 1.6  $\mu\text{m}$  can be attributed only to the  $^3F_3 \rightarrow ^3H_4$  transition and was successfully fit with a single exponential function with a lifetime of 0.27 ms. In comparison with the literature data of  $\text{Pr}^{3+}$ -doped chalcogenide-selenide glasses, the measured lifetime of 0.27 ms for  $^3F_3$  level obtained in this work is in good agreement with the measured lifetime of 0.25 ms for the  $^3F_3$  level [15]. Thus, the measured fast decay at 7.4  $\mu\text{m}$  and the decay measured at 1.6  $\mu\text{m}$  have similar time constants. These results indicate that both emissions originate from the same  $^3F_3$  manifold. To the Authors' best knowledge, this is the first observation of 7.4  $\mu\text{m}$  emission attributed mainly to  $^3F_3 \rightarrow ^3F_2$  in a  $\text{Pr}^{3+}$  selenide chalcogenide fiber and supports the observation by Churbanov et al. of a similar emission in  $\text{Pr}^{3+}$ -doped bulk selenide-chalcogenide glass [19]. It should be pointed out that, using this same transition, room temperature laser action at 7.2  $\mu\text{m}$  in  $\text{Pr}^{3+}$ :  $\text{LaCl}_3$  was obtained [37]. It is well known that rapid thermalization takes place within each of the two pairs of closely-lying upper states [ $^3F_4$  with  $^3F_3$ ] and [ $^3F_2$  with  $^3H_6$ ]  $\text{Pr}^{3+}$  levels in the chalcogenide glass host, with occupancy in the two lower states of at least  $\sim 90\%$  [15,16]. Thus, under pumping at 1.47  $\mu\text{m}$  from the ground state to the  $^3F_4$  level, most of the ions will immediately

drop down to level  $^3F_3$ , whilst only a small fraction of ions will occupy the  $^3F_2$  level. Therefore, a laser operating on the  $^3F_3 \rightarrow ^3F_2$  transitions, in a selenide-chalcogenide glass host, should act as a true four-level laser system. Additionally, it is noted that the minimum loss in a selenide-chalcogenide glass has been recorded at approximately  $6.6 \mu\text{m}$ , which further predestines the  $^3F_3 \rightarrow ^3F_2$  transition for a successful realization of the first chalcogenide glass fiber laser operating at a wavelength exceeding  $4 \mu\text{m}$  [47].

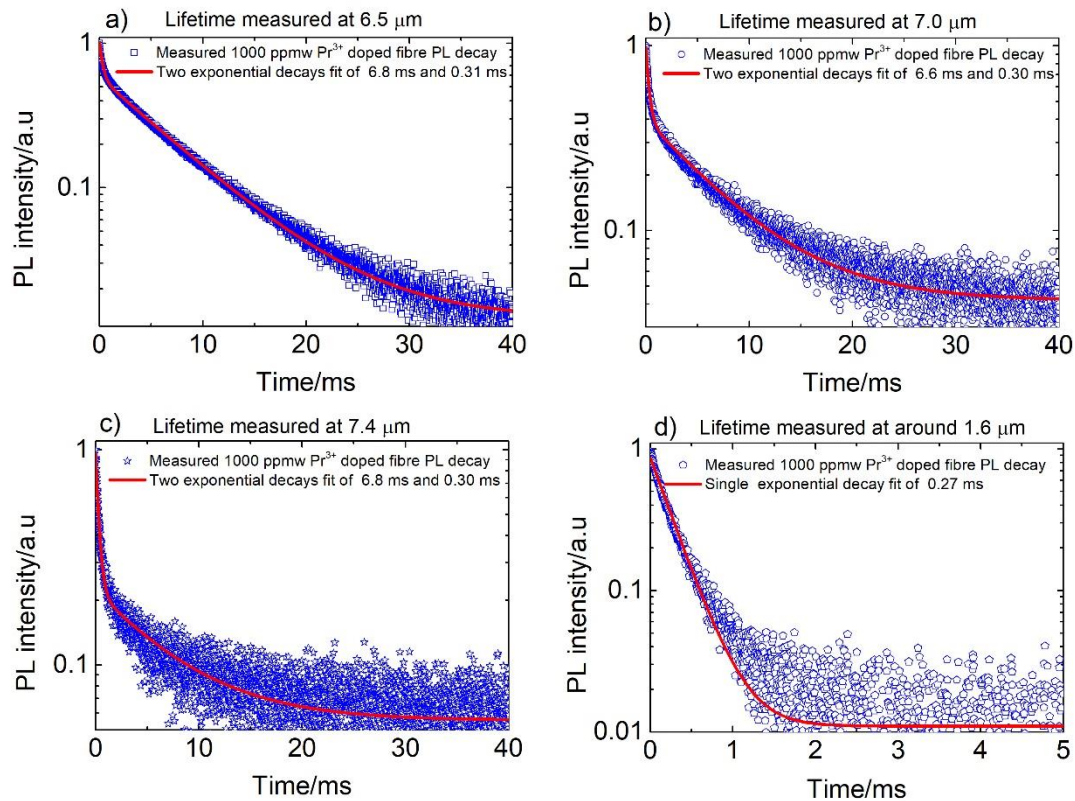


**Figure 7.** Measured photoluminescence decay at: (a)  $6.5 \mu\text{m}$ ; (b)  $7 \mu\text{m}$ ; (c)  $7.4 \mu\text{m}$  and (d)  $1.6 \mu\text{m}$  in 1000 ppmw  $\text{Pr}^{3+}$ -doped GeAsGaSe chalcogenide glass fiber. The laser excitation was at  $1.47 \mu\text{m}$ .

#### 4. Conclusions

In this paper, mid-infrared spontaneous emission sources based on  $\text{Pr}^{3+}$ -doped chalcogenide fiber were experimentally investigated. The experimental results obtained confirm that the developed spontaneous emission source made of  $\text{Pr}^{3+}$ -doped chalcogenide fiber delivers maximum output power of at least 1 mW within the spectral region  $3.5\text{--}8 \mu\text{m}$  under pumping employing easily commercially available laser diodes operating at  $1.470 \mu\text{m}$ ,  $1.511 \mu\text{m}$  and  $1.690 \mu\text{m}$ . Moreover, emission in the region  $6.2\text{--}8.0 \mu\text{m}$  was measured for the first time in a  $\text{Pr}^{3+}$  chalcogenide selenide fiber, to the Authors' best knowledge. Measured lifetimes at  $7.4 \mu\text{m}$  and  $1.6 \mu\text{m}$  confirm that the recorded emission originates from the  $^3F_3$  level. This observation may also be an important step towards the first realization of mid-infrared fiber laser operating at wavelengths beyond  $4 \mu\text{m}$ , because experimental results indicate that lasing based on the  $^3F_3 \rightarrow ^3F_2$  transition could operate as a four-level laser system in a selenide-chalcogenide glass host.

**Author Contributions:** Conceptualization, L.S. and S.S.; Methodology, L.S., Z.T., D.J., M.S., J.N., D.F., M.F., T.M.B., A.B.S., and S.S.; Validation, L.S., Z.T., D.J., M.S., J.N., D.F., M.F., T.M.B., A.B.S., and S.S.; Formal analysis, L.S., T.M.B., A.B.S., and S.S.; Writing—original draft preparation, L.S., and S.S.; Writing—review and editing, L.S., T.M.B., A.B.S., and S.S. All authors have read and agreed to the published version of the manuscript.

**Funding:** This Project has received funding from the European Union's Horizon 2020 Research and Innovation Programme under the Marie Skłodowska-Curie grant agreement No. 665778 (National Science Centre, Poland,

Polonez Fellowship 2016/21/P/ST7/03666). The authors wish to thank also Wrocław University of Science and Technology for financial support (049U/0032/19).

**Acknowledgments:** In this section you can acknowledge any support given which is not covered by the author contribution or funding sections. This may include administrative and technical support, or donations in kind (e.g., materials used for experiments).

**Conflicts of Interest:** The authors declare no conflict of interest.

## References

1. Jackson, S.D. Towards high-power mid-infrared emission from a fibre laser. *Nat. Photonics* **2012**, *6*, 423–431. [[CrossRef](#)]
2. Walsh, B.M.; Lee, H.R.; Barnes, N.P. Mid infrared lasers for remote sensing applications. *J. Lumin.* **2016**, *169*, 400–405. [[CrossRef](#)]
3. Woodward, R.I.; Majewski, M.R.; Hudson, D.D.; Jackson, S.D. Swept-wavelength mid-infrared fiber laser for real-time ammonia gas sensing. *APL Photonics* **2019**, *4*, 020801. [[CrossRef](#)]
4. Petersen, C.R.; Prtljaga, N.; Farries, M.; Ward, J.; Napier, B.; Lloyd, G.R.; Nallala, J.; Stone, N.; Bang, O. Mid-infrared multispectral tissue imaging using a chalcogenide fiber supercontinuum source. *Opt. Lett.* **2018**, *43*, 999–1002. [[CrossRef](#)] [[PubMed](#)]
5. Seddon, A.B.; Tang, Z.; Furniss, D.; Sujecki, S.; Benson, T.M. Progress in rare-earth-doped mid-infrared fiber lasers. *Opt. Express* **2010**, *18*, 26704–26719. [[CrossRef](#)] [[PubMed](#)]
6. Maes, F.; Fortin, V.; Poulain, S.; Poulain, M.; Carrée, J.-Y.; Bernier, M.; Vallée, R. Room-temperature fiber laser at 3.92  $\mu\text{m}$ . *Optica* **2018**, *5*, 761–764. [[CrossRef](#)]
7. Majewski, M.R.; Woodward, R.I.; Carreé, J.-Y.; Poulain, S.; Poulain, M.; Jackson, S.D. Emission beyond 4  $\mu\text{m}$  and mid-infrared lasing in a dysprosium-doped indium fluoride (InF<sub>3</sub>) fiber. *Opt. Lett.* **2018**, *43*, 1926–1929. [[CrossRef](#)] [[PubMed](#)]
8. Schneider, J. Fluoride fibre laser operating at 3.9  $\mu\text{m}$ . *Electron. Lett.* **1995**, *31*, 1250–1251. [[CrossRef](#)]
9. Jayasuriya, D.; Petersen, C.R.; Furniss, D.; Markos, C.; Tang, Z.; Habib, M.S.; Bang, O.; Benson, T.M.; Seddon, A.B. Mid-IR supercontinuum generation in birefringent, low loss, ultra-high numerical aperture Ge-As-Se-Te chalcogenide step-index fiber. *Opt. Mater. Express* **2019**, *9*, 2617–2629. [[CrossRef](#)]
10. Petersen, C.R.; Engelsholm, R.D.; Markos, C.; Brilland, L.; Caillaud, C.; Trolès, J.; Bang, O. Increased mid-infrared supercontinuum bandwidth and average power by tapering large-mode-area chalcogenide photonic crystal fibers. *Opt. Express* **2017**, *25*, 15336–15348. [[CrossRef](#)]
11. Bernier, M.; Fortin, V.; El-Amraoui, M.; Messaddeq, Y.; Vallée, R. 3.77  $\mu\text{m}$  fiber laser based on cascaded Raman gain in a chalcogenide glass fiber. *Opt. Lett.* **2014**, *39*, 2052–2055. [[CrossRef](#)] [[PubMed](#)]
12. Tang, Z.; Furniss, D.; Fay, M.; Sakr, H.; Sójka, L.; Neate, N.; Weston, N.; Sujecki, S.; Benson, T.M.; Seddon, A.B. Mid-infrared photoluminescence in small-core fiber of praseodymium-ion doped selenide-based chalcogenide glass. *Opt. Mater. Express* **2015**, *5*, 870–886. [[CrossRef](#)]
13. Karaksina, E.V.; Shiryayev, V.S.; Churbanov, M.F.; Anashkina, E.A.; Kotereva, T.V.; Snopatin, G.E. Core-clad Pr(3+)-doped Ga(In)-Ge-As-Se-(I) glass fibers: Preparation, investigation, simulation of laser characteristics. *Opt. Mater.* **2017**, *72*, 654–660. [[CrossRef](#)]
14. Pelé, A.L.; Braud, A.; Doualan, J.L.; Starecki, F.; Nazabal, V.; Chahal, R.; Boussard-Plédel, C.; Bureau, B.; Moncorgé, R.; Camy, P. Dy<sup>3+</sup> doped GeGaSbS fluorescent fiber at 4.4  $\mu\text{m}$  for optical gas sensing: Comparison of simulation and experiment. *Opt. Mater.* **2016**, *61*, 37–44.
15. Shaw, L.B.; Cole, B.; Thielen, P.A.; Sanghera, J.S.; Aggarwal, I.D. Mid-wave IR and long-wave IR laser potential of rare-earth doped chalcogenide glass fiber. *IEEE J. Quantum Electron.* **2001**, *37*, 1127–1137. [[CrossRef](#)]
16. Shaw, L.B.; Harbison, B.B.; Cole, B.; Sanghera, J.S.; Aggarwal, I.D. Spectroscopy of the IR transitions in Pr<sup>3+</sup> doped heavy metal selenide glasses. *Opt. Express* **1997**, *1*, 87–96. [[CrossRef](#)] [[PubMed](#)]
17. Chahal, R.; Starecki, F.; Doualan, J.-L.; Nèmec, P.; Trapananti, A.; Prestipino, C.; Tricot, G.; Boussard-Plédel, C.; Michel, K.; Braud, A.; et al. Nd<sup>3+</sup>:Ga-Ge-Sb-S glasses and fibers for luminescence in mid-IR: Synthesis, structural characterization and rare earth spectroscopy. *Opt. Mater. Express* **2018**, *8*, 1650–1671. [[CrossRef](#)]
18. Sanghera, J.S.; Shaw, L.B.; Aggarwal, I.D. Chalcogenide Glass-Fiber-Based Mid-IR Sources and Applications. *IEEE J. Sel. Top. Quantum Electron.* **2009**, *15*, 114–119. [[CrossRef](#)]

19. Churbanov, M.F.; Denker, B.I.; Galagan, B.I.; Koltashev, V.V.; Plotnichenko, V.G.; Sverchkov, S.E.; Sukhanov, M.V.; Velmuzhov, A.P. Peculiarities of 1.6–7.5  $\mu\text{m}$   $\text{Pr}^{3+}$  luminescence in  $\text{Ge}_{36}\text{Ga}_5\text{Se}_{59}$  glass. *Opt. Mater. Express* **2019**, *9*, 4154–4164. [[CrossRef](#)]
20. Starecki, F.; Abdellaoui, N.; Braud, A.; Doualan, J.-L.; Boussard-Plédel, C.; Bureau, B.; Camy, P.; Nazabal, V. 8  $\mu\text{m}$  luminescence from a  $\text{Tb}^{3+}$   $\text{GaGeSbSe}$  fiber. *Opt. Lett.* **2018**, *43*, 1211–1214. [[CrossRef](#)]
21. Starecki, F.; Braud, A.; Abdellaoui, N.; Doualan, J.-L.; Boussard-Plédel, C.; Bureau, B.; Camy, P.; Nazabal, V. 7 to 8  $\mu\text{m}$  emission from  $\text{Sm}^{3+}$  doped selenide fibers. *Opt. Express* **2018**, *26*, 26462–26469. [[CrossRef](#)] [[PubMed](#)]
22. Seddon, A.B.; Furniss, D.; Tang, Z.Q.; Sojka, L.; Benson, T.M.; Caspary, R.; Sujecki, S. True mid-infrared  $\text{Pr}^{3+}$  absorption cross-section in a selenide-chalcogenide host-glass. In Proceedings of the 2016 18th International Conference on Transparent Optical Networks (ICTON), Trento, Italy, 11–14 July 2016; pp. 1–6.
23. Sujecki, S.; Sojka, L.; Pawlik, E.; Anders, K.; Piramidowicz, R.; Tang, Z.; Furniss, D.; Barney, E.; Benson, T.; Seddon, A. Numerical analysis of spontaneous mid-infrared light emission from terbium ion doped multimode chalcogenide fibers. *J. Lumin.* **2018**, *199*, 112–115. [[CrossRef](#)]
24. Starecki, F.; Morais, S.; Chahal, R.; Boussard-Plédel, C.; Bureau, B.; Palencia, F.; Lecoutre, C.; Garrabos, Y.; Marre, S.; Nazabal, V. IR emitting  $\text{Dy}^{3+}$  doped chalcogenide fibers for in situ  $\text{CO}_2$  monitoring in high pressure microsystems. *Int. J. Greenh. Gas Control* **2016**, *55*, 36–41. [[CrossRef](#)]
25. Ari, J.; Starecki, F.; Boussard-Plédel, C.; Ledemi, Y.; Messaddeq, Y.; Doualan, J.-L.; Braud, A.; Bureau, B.; Nazabal, V. Co-doped  $\text{Dy}^{3+}$  and  $\text{Pr}^{3+}$   $\text{Ga}_5\text{Ge}_{20}\text{Sb}_{10}\text{Sb}_{65}$  fibers for mid-infrared broad emission. *Opt. Lett.* **2018**, *43*, 2893–2896. [[CrossRef](#)]
26. Starecki, F.; Braud, A.; Doualan, J.-L.; Ari, J.; Boussard-Plédel, C.; Michel, K.; Nazabal, V.; Camy, P. All-optical carbon dioxide remote sensing using rare earth doped chalcogenide fibers. *Opt. Lasers Eng.* **2019**, *122*, 328–334. [[CrossRef](#)]
27. Shiryaev, V.S.; Karaksina, E.V.; Kotereva, T.V.; Churbanov, M.F.; Velmuzhov, A.P.; Nezhdanov, A.V. Special pure  $\text{Pr}^{3+}$  doped  $\text{Ga}_3\text{Ge}_{31}\text{As}_{18}\text{Se}_{48}$  glass for active mid-IR optics. *J. Lumin.* **2019**, *209*, 225–231. [[CrossRef](#)]
28. Sourková, P.; Frumarova, B.; Frumar, M.; Nemeč, P.; Kincl, M.; Nazabal, V.; Moizan, V.; Doualan, J.-L.; Moncorgé, R. Spectroscopy of infrared transitions of  $\text{Pr}^{3+}$  ions in Ga–Ge–Sb–Se glasses. *J. Lumin.* **2009**, *129*, 1148–1153. [[CrossRef](#)]
29. Sakr, H.; Furniss, D.; Tang, Z.; Sojka, L.; Moneim, N.A.; Barney, E.; Sujecki, S.; Benson, T.M.; Seddon, A.B. Superior photoluminescence (PL) of  $\text{Pr}^{3+}$ -In, compared to  $\text{Pr}^{3+}$ -Ga, selenide-chalcogenide bulk glasses and PL of optically-clad fiber. *Opt. Express* **2014**, *22*, 21236–21252. [[CrossRef](#)]
30. Shiryaev, V.S.; Karaksina, E.V.; Kotereva, T.V.; Churbanov, M.F.; Velmuzhov, A.P.; Sukhanov, M.V.; Ketkova, L.A.; Zernova, N.S.; Plotnichenko, V.G.; Koltashev, V.V. Preparation and investigation of  $\text{Pr}^{3+}$ -doped Ge–Sb–Se–In–I glasses as promising material for active mid-infrared optics. *J. Lumin.* **2017**, *183*, 129–134. [[CrossRef](#)]
31. Ma, C.; Guo, H.; Xu, Y.; Wu, Z.; Li, M.; Jia, X.; Nie, Q. Effect of glass composition on the physical properties and luminescence of  $\text{Pr}^{3+}$  ion-doped chalcogenide glasses. *J. Am. Ceram. Soc.* **2019**, *102*, 6794–6801. [[CrossRef](#)]
32. Liu, Z.; Bian, J.; Huang, Y.; Xu, T.; Wang, X.; Dai, S. Fabrication and characterization of mid-infrared emission of  $\text{Pr}^{3+}$  doped selenide chalcogenide glasses and fibres. *RSC Adv.* **2017**, *7*, 41520–41526. [[CrossRef](#)]
33. Palma, G.; Falconi, M.C.; Starecki, F.; Nazabal, V.; Ari, J.; Bodiou, L.; Charrier, J.; Dumeige, Y.; Baudet, E.; Prudenžano, F. Design of praseodymium-doped chalcogenide micro-disk emitting at 4.7  $\mu\text{m}$ . *Opt. Express* **2017**, *25*, 7014–7030. [[CrossRef](#)] [[PubMed](#)]
34. Shpotyuk, Y.; Boussard-Plédel, C.; Nazabal, V.; Chahal, R.; Ari, J.; Pavlyk, B.; Cebulski, J.; Doualan, J.L.; Bureau, B. Ga-modified  $\text{As}_2\text{Se}_3$ –Te glasses for active applications in IR photonics. *Opt. Mater.* **2015**, *46*, 228–232. [[CrossRef](#)]
35. Bodiou, L.; Starecki, F.; Lemaitre, J.; Nazabal, V.; Doualan, J.-L.; Baudet, E.; Chahal, R.; Gutierrez-Arroyo, A.; Dumeige, Y.; Hardy, I.; et al. Mid-infrared guided photoluminescence from integrated  $\text{Pr}^{3+}$ -doped selenide ridge waveguides. *Opt. Mater.* **2018**, *75*, 109–115. [[CrossRef](#)]
36. Walsh, B.M.; Hommerich, U.; Yoshikawa, A.; Toncelli, A. Mid-infrared spectroscopy of Pr-doped materials. *J. Lumin.* **2018**, *197*, 349–353. [[CrossRef](#)]
37. Bowman, S.R.; Shaw, L.B.; Feldman, B.J.; Ganem, J. A 7- $\mu\text{m}$  praseodymium-based solid-state laser. *IEEE J. Quantum Electron.* **1996**, *32*, 646–649. [[CrossRef](#)]
38. Bowman, S.R.; Ganem, J.; Feldman, B.J.; Kueny, A.W. Infrared laser characteristics of praseodymium-doped lanthanum trichloride. *IEEE J. Quantum Electron.* **1994**, *30*, 2925–2928. [[CrossRef](#)]

39. Yu, D.; Ballato, J.; Riman, R.E. The Temperature-Dependence of Multiphonon Relaxation of Rare-Earth Ions in Solid-State Hosts. *J. Phys. Chem. C Nanomater. Interfaces* **2016**, *120*, 9958–9964. [[CrossRef](#)]
40. Choi, Y.G.; Park, B.J.; Kim, K.H.; Heo, J. Pr<sup>3+</sup>- and Pr<sup>3+</sup>/Er<sup>3+</sup>-doped selenide glasses for potential 1.6 μm optical amplifier materials. *Etri. J.* **2001**, *23*, 97–105. [[CrossRef](#)]
41. Choi, Y.G.; Kim, K.H.; Park, B.J.; Heo, J. 1.6 μm emission from Pr<sup>3+</sup>:(<sup>3</sup>F<sub>3</sub>,<sup>3</sup>F<sub>4</sub>)→<sup>3</sup>H<sub>4</sub> transition in Pr<sup>3+</sup>- and Pr<sup>3+</sup>/Er<sup>3+</sup>-doped selenide glasses. *Appl. Phys. Lett.* **2001**, *78*, 1249–1251. [[CrossRef](#)]
42. Choi, Y.G.; Seo, Y.B.; Heo, J. Enhancement in lifetimes of the Pr<sup>3+</sup>: 1.6 μm emission in Ge-Ga-As-Se glasses with CsBr addition. *J. Mater. Sci. Lett.* **2003**, *22*, 795–798. [[CrossRef](#)]
43. Han, Y.S.; Heo, J. Midinfrared emission properties of Pr<sup>3+</sup>-doped chalcogenide glasses at cryogenic temperature. *J. Appl. Phys.* **2003**, *93*, 8970–8974. [[CrossRef](#)]
44. Sujecki, S.; Sojka, L.; Beres-Pawlik, E.; Anders, K.; Piramidowicz, R.; Tang, Z.; Furniss, D.; Barney, E.; Benson, T.; Seddon, A. Experimental and numerical investigation to rationalize both near-infrared and mid-infrared spontaneous emission in Pr<sup>3+</sup> doped selenide-chalcogenide fiber. *J. Lumin.* **2019**, *209*, 14–20. [[CrossRef](#)]
45. Sojka, L.; Tang, Z.; Jayasuriya, D.; Shen, M.; Furniss, D.; Barney, E.; Benson, T.M.; Seddon, A.B.; Sujecki, S. Ultra-broadband mid-infrared emission from a Pr<sup>3+</sup>/Dy<sup>3+</sup> co-doped selenide-chalcogenide glass fiber spectrally shaped by varying the pumping arrangement [Invited]. *Opt. Mater. Express* **2019**, *9*, 2291–2306. [[CrossRef](#)]
46. Kamensky, V.A.; Scripachev, I.V.; Snopatin, G.E.; Pushkin, A.A.; Churbanov, M.F. High-power As-S glass fiber delivery instrument for pulse YAG:Er laser radiation. *Appl. Opt.* **1998**, *37*, 5596–5599. [[CrossRef](#)]
47. Tang, Z.; Shiryaev, V.S.; Furniss, D.; Sojka, L.; Sujecki, S.; Benson, T.M.; Seddon, A.B.; Churbanov, M.F. Low loss Ge-As-Se chalcogenide glass fiber, fabricated using extruded preform, for mid-infrared photonics. *Opt. Mater. Express* **2015**, *5*, 1722–1737. [[CrossRef](#)]



© 2020 by the authors. Licensee MDPI, Basel, Switzerland. This article is an open access article distributed under the terms and conditions of the Creative Commons Attribution (CC BY) license (<http://creativecommons.org/licenses/by/4.0/>).